Non-unique Equilibria in Wind Turbine Models

Ian A. Hiskens, *Fellow, IEEE*
Department of Electrical Engineering and Computer Science
University of Michigan, Ann Arbor

***Abstract*—Accurate dynamic models of wind turbine generators are extremely important for assessing the effect of wind generation on power system dynamic performance. The paper considers a generic model for doubly-fed induction generator (type-3) wind turbines. It is shown that two of its modules, those associated with converter control and pitch control, duplicate an integrator that seeks to drive frequency error to zero. As a consequence of these duplicate integrators, the set of equations describing steady-state conditions is under-determined. Equilibria define a 1-manifold (curve) rather than the usual point solutions. It is shown that if the duplicated integrators are switched in unison, then pre- and post-disturbance equilibria will coincide. However if switching of the duplicated integrators is not coordinated, then post-disturbance transients will generically settle to a steady-state that differs from pre-disturbance conditions. These conclusions are illustrated using a standard WECC test case.**

***Index Terms*—Wind turbine modelling; ill-posed systems; under-determined equilibria; switched systems.**

I. Introduction

WIND turbine generator (WTG) technology is vastly different to traditional synchronous generators [1], so the dynamic characteristics of power systems may alter as wind generation supplants an ever increasing amount of traditional generation [2]. Accurate modelling of the dynamic behaviour of WTGs is therefore extremely important for understanding the impact of large-scale wind generation on system dynamic performance [3]. Accordingly, the modelling of WTGs has received considerable attention, see for example [2], [4], [5], [6] and references therein.

Turbine manufacturers routinely develop and maintain accurate models for their products, though disclosure of those models is highly restricted. In some cases they have released models that describe functionally similar behaviour [7], though such practise is not common. Regional reliability organizations need to exchange models and data that are relevant to their jurisdiction. This has motivated the development of generic models that can be used to capture the functional characteristics of a wide variety of WTGs [8], [9], [10].

This paper focusses on doubly-fed induction generator (DFIG) wind turbine models, which are also known as type-3 WTGs. These wind turbines are currently the primary technology for new wind-farm developments. However, the modelling issues that are addressed in this paper also afflict some full converter (type-4) wind-turbine models [10].

The electrical characteristics of type-3 WTGs are governed by interactions between a wound-rotor induction machine and a back-to-back inverter. The inverter excites the rotor of the induction machine with a variable AC source. This provides control of the rotor flux frequency, enabling the rotor shaft frequency to optimally track wind speed [1]. The inverter response time is very fast relative to electromechanical time constants. As a result, the natural dynamics of the induction machine are largely masked from the power system. The dynamic behaviour of a type-3 WTG, as seen from the grid, is therefore dominated by controller response rather than physical characteristics. This is in marked contrast to traditional synchronous generators, where behaviour is governed by device physics.

The studies presented in this paper focus on the WECC generic type-3 model [9], [10], which is effectively the same as the GE model [7]. This model has been chosen because it is widely used, and is indicative of type-3 models that are generally available. All such generic models are an approximation of the actual dynamics exhibited by a WTG. It is important, though, that such approximations reflect the physical reality of the modelled device.

The paper is organized as follows. Section II provides an overview of the WECC type-3 WTG model. It is shown in Section III that switching associated with duplicate integrators will result in pre- and post-disturbance equilibria not coinciding. A remedy for this anomalous behaviour is also proposed. Conclusions are presented in Section IV.

II. Type-3 WTG model

The WECC type-3 wind turbine generator model is defined in [9], [10]. The complete WTG model is divided into four functional blocks, as indicated in Figure 1. This paper is primarily concerned with the dynamics of the converter control module WT3E and the pitch control module WT3P. Accordingly, only those two modules are described in detail in the following analysis.

A. Converter control module WT3E

The converter control module is composed of separate active and reactive power control functions. Reactive power control is very fast, due to the power electronic converter. This paper focuses on the slower dynamics associated with interactions between active power (torque) control and pitch control. Therefore only the active power model, which is shown in Figure 2, will be discussed. Full details of the reactive power controller are provided in [9], [10].

The non-windup (anti-windup) limits on the PI block in the centre of Figure 2 are driven by the non-windup P_{max}/P_{min}

Research supported by the Department of Energy through grant DE-EE0001382.

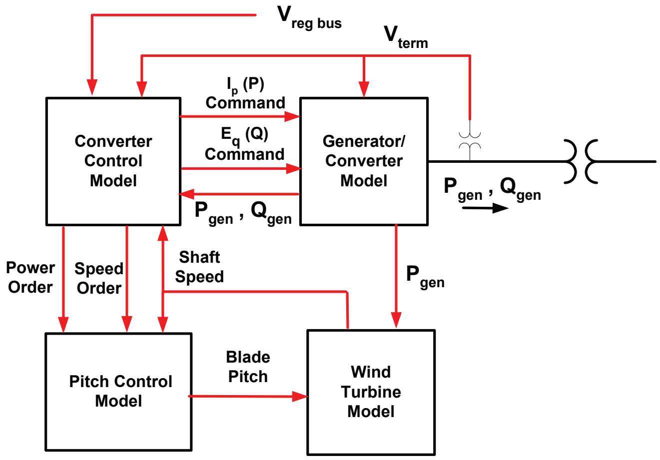

Fig. 1. Type-3 WTG dynamic model connectivity, from [9], [10].

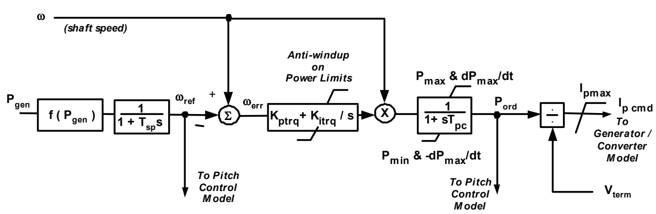

Fig. 2. Converter control model WT3E, from [9], [10].

limits associated with the P_{ord} lag block. The model documentation stipulates that:

(i) If P_{ord} is on its P_{max} limit and ω_{err} (the input to the PI block) is positive, then the K_{itrq}-integrator is blocked, i.e., the state T_ω of that integrator is frozen.

(ii) If P_{ord} is on the P_{min} limit and ω_{err} is negative, then the K_{itrq}-integrator state is frozen.

This form of non-windup limit is unusual. It has been shown in [11], [12] that such non-windup logic can result in switching deadlock [13].

The PI controller of the WT3E block contributes the switched differential equation,

$$\frac{dT_\omega}{dt} = K_{itrq}(\omega - \omega_{ref}) \times y_{s1} \tag{1}$$

where the auxiliary variable y_{s1} equals 0 when the conditions for blocking the K_{itrq}-integrator are satisfied and 1 otherwise.

B. Pitch control module WT3P

The pitch control module WT3P is shown in Figure 3. Of particular importance is the implementation of the non-windup limiter on the pitch angle θ. As stated in the model documentation,

> "The Pitch Control and Pitch Compensation integrators are non-windup integrators as a function of the pitch, i.e., the inputs of these integrators are set to zero when the pitch is in limits (PI_{max} or PI_{min}) and the integrator input tends to force the pitch command further against its limit."

This blocking philosophy is similar to that employed in the converter control module WT3E, as discussed in Section II-A.

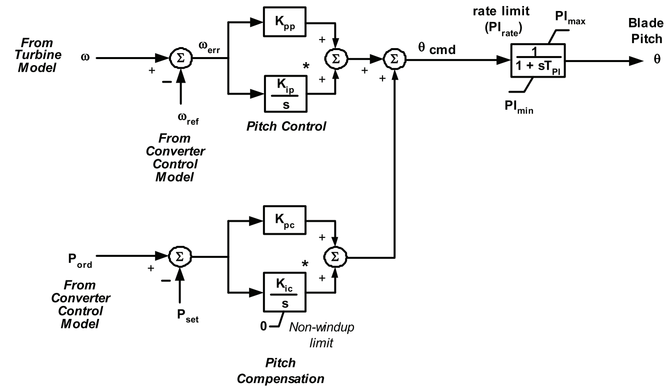

Fig. 3. Pitch control model WT3P, from [9], [10].

It should again be mentioned that such blocking can result in switching deadlock [12].

The pitch control integrator contributes the switched differential equation,

$$\frac{dx_p}{dt} = K_{ip}(\omega - \omega_{ref}) \times y_{s2} \tag{2}$$

where the auxiliary variable y_{s2} equals 0 when the conditions for blocking the pitch control integrator are satisfied and 1 otherwise.

III. Equilibrium Conditions

A. Duplicate integrators

It is clear from (1) and (2) that the WT3E and WT3P modules duplicate an integrator, with each seeking to drive the frequency error $(\omega - \omega_{ref})$ to zero. In determining steady-state conditions, these two integrators contribute the exact same algebraic equation,

$$\omega - \omega_{ref} = 0 \tag{3}$$

but introduce two variables T_ω and x_p. The resulting steady-state description is therefore under-determined, implying that equilibria lie along a 1-manifold.

For well-posed dynamical models, the post-disturbance steady-state should match the pre-disturbance (initial) equilibrium when pre- and post-disturbance parameter sets are identical. This is generically not the case for the WECC type-3 WTG model, because of the duplicate integrators.

This indeterminacy is resolved when the duplicate integrators (1) and (2) remain unblocked over the entire time horizon. In that case, the integrator states can be written in integral form,

$$T_\omega(t) = T_\omega^o + K_{itrq} \int_0^t \big(\omega(\tau) - \omega_{ref}(\tau)\big) d\tau \tag{4}$$

$$x_p(t) = x_p^o + K_{ip} \int_0^t \big(\omega(\tau) - \omega_{ref}(\tau)\big) d\tau \tag{5}$$

where T_ω^o and x_p^o are the initial values for the respective states. Equating the integrals in (4) and (5) gives the affine relationship,

$$x_p(t) = \frac{K_{ip}}{K_{itrq}} T_w(t) + \left(x_p^0 - \frac{K_{ip} T_w^0}{K_{itrq}} \right) \tag{6}$$

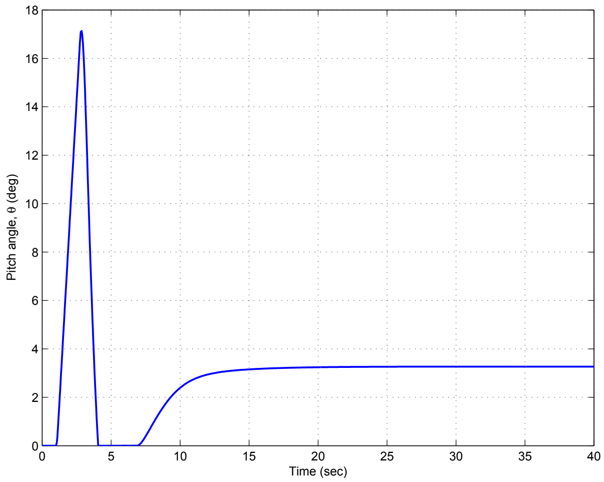

(a) Pitch angle θ.

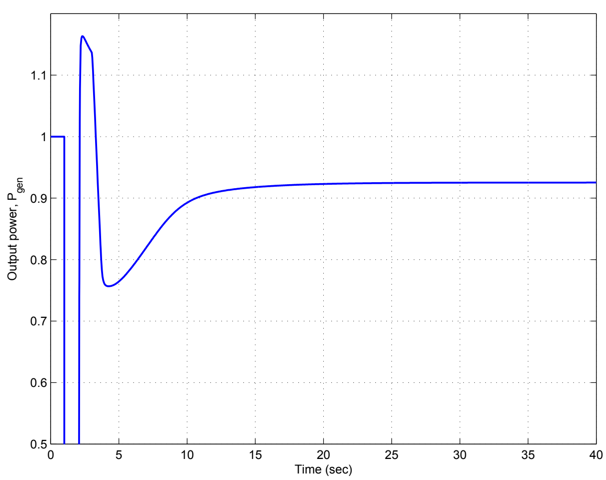

(b) Output power P_{gen}.

Fig. 4. Large disturbance response. No coordination between integrators.

which implies that any variation in $T_\omega(t)$ will be matched by a corresponding variation in $x_p(t)$. This relationship provides the extra equation required to uniquely determine the post-disturbance steady-state, and in fact implies that if all parameters remain unchanged, the system will evolve to a steady-state that exactly matches the initialization point.

The assumption that the duplicate integrators remain unblocked for all time is seldom true, however. Blocking of one or other of the integrators will alter the corresponding integral term in (4) or (5), invalidating the relationship (6). Under such conditions, it becomes impossible for both T_ω and x_p to evolve back to their initial values. Consequently, the system will settle to a post-disturbance steady-state that cannot equal the initial point, even though the parameters of the system are unchanged.

B. Example: uncoordinated integrator switching

The WECC test system given in [9], [12] can be used to illustrate the effect of the duplicate integrators on post-disturbance equilibrium conditions. Whilst the behaviour of interest occurs for the default parameter set, in order to provide

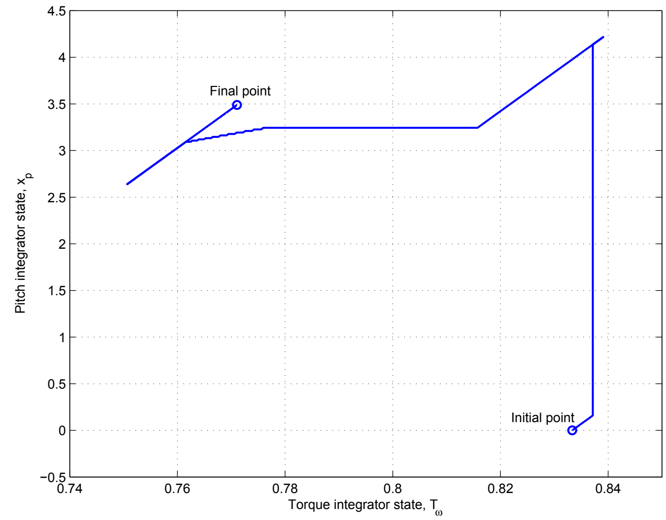

Fig. 5. Relationship between $T_\omega(t)$ and $x_p(t)$. No coordination between integrators.

a clearer illustration, fault impedance has been increased to 0.02 pu, and the fault-on time extended to 1 s. This is representative of a distant, slowly-cleared fault, an event that is not atypical for sub-transmission networks where many wind-farms are located.

The responses of the pitch angle and output power are shown in Figure 4. Notice that the pitch angle evolves to a steady-state value of 3.3 deg, even though it was initialized at 0 deg. Of even greater concern is the fact that the output power only recovers to 0.925 pu, after being initialized at 1.0 pu. This 7.5% drop in power, when accumulated across multiple wind-farms, could amount to a significant reduction in generation. That deficit in wind-power output would result in a frequency decline, causing governors of frequency-regulating plant to respond. Consequently, the resulting post-event steady-state achieved by simulation would not reflect reality.

Figure 5 shows the relationship between T_ω and x_p. These two states initially follow a straight line given by (6), with the states reaching the point $(T_\omega, x_p) = (0.837, 0.160)$, where the T_ω-integrator becomes blocked. The x_p-integrator continues to evolve, with (T_ω, x_p) reaching $(0.837, 4.137)$ where T_ω becomes unblocked. The states then move in unison along a straight line defined by (6), initially increasing to $(0.839, 4.218)$ before decreasing to $(0.816, 3.243)$ where the x_p-integrator becomes blocked. From this point, T_ω evolves until encountering $(0.776, 3.243)$. Over the subsequent period of staircase behaviour, the x_p-integrator successively blocks and unblocks due to a hysteresis band. The states emerge from this period at $(0.762, 3.094)$, and evolve to their final steady-state along a straight line that is again dictated by (6).

Notice that whenever both integrators are free, behaviour is described by the affine relationship (6), with slope given by K_{ip}/K_{itrq}. But also notice that the offset constant is different for each of those sections. Once either integrator blocks, the states can never return to their original starting equilibrium point.

This situation is a consequence of a model structure that

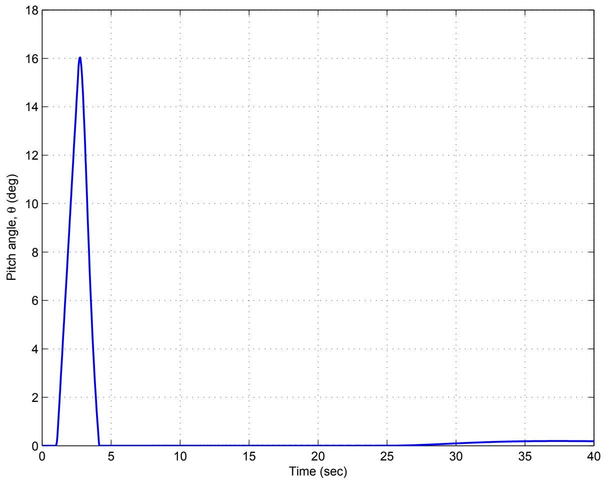

(a) Pitch angle θ.

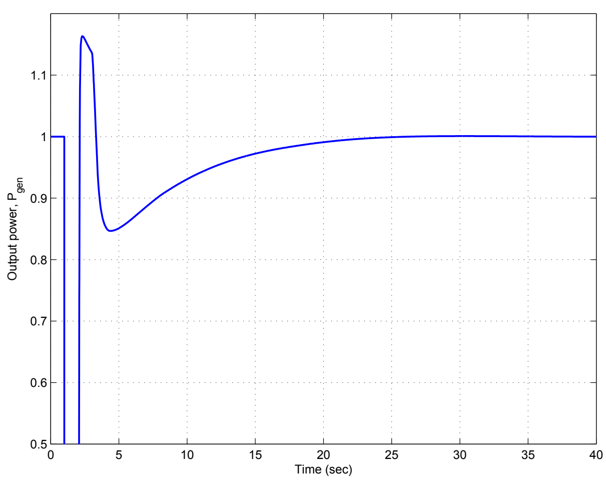

(b) Output power P_{gen}.

Fig. 6. Large disturbance response. Synchronized switching of integrators.

involves disparate switching of duplicate integrators. Actual WTGs controls do not have such a structure, so real WTGs do not exhibit such abnormal behaviour. Nevertheless, the behaviour is of concern to utilities engineers who are required to use these generic models.

C. Coordinated switching of integrators

The non-uniqueness in equilibria that is inherent in duplicate integrators only affects the post-disturbance steady-state when the integrators switch asynchronously. That issue can be addressed by forcing the duplicate integrators to switch in unison. Referring to (1), (2), the desired strategy can be achieved by introducing the modification

$$\frac{dT_\omega}{dt} = K_{itrq}(\omega - \omega_{ref}) \times y_{s1} \times y_{s2} \tag{7}$$

$$\frac{dx_p}{dt} = K_{ip}\big(\omega - \omega_{ref}\big) \times y_{s1} \times y_{s2} \tag{8}$$

which ensures each integrator is subject to exactly the same switching conditions.

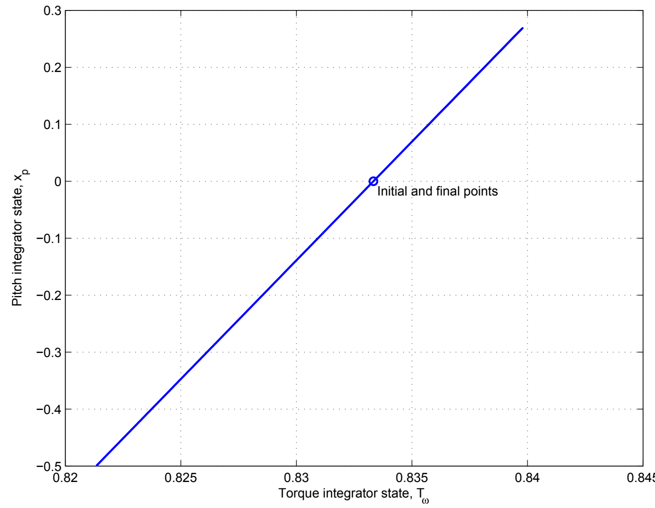

Fig. 7. Relationship between $T_\omega(t)$ and $x_p(t)$. Synchronized switching of integrators.

D. Example: synchronously-switched integrators

Repeating the example of Section III-B, with the modification (7)-(8) implemented, gave the pitch angle and output power responses shown in Figure 6. The output power has recovered to its pre-disturbance value, while the pitch angle is close to its original value. In the latter case, pitch angle dynamic response is very slow when the angle is close to zero, hence it has not quite stabilized. It does, in fact, settle to zero by around 100 s.

The behaviour of T_ω and x_p is shown in Figure 7. It is clear in this case that T_ω and x_p satisfy the affine relationship (6) for all time. Accordingly, the pre- and post-disturbance equilibria coincide.

IV. Conclusions

The paper has considered the modelling of doubly-fed induction generator (type-3) wind turbines, and has focussed on the WECC type-3 wind turbine generator model. Two of the modules within that model, the converter controller and the pitch controller, have integrators that provide the same function, namely to drive the frequency error to zero. It is shown in the paper that these duplicate integrators add two variables to the steady-state description, but only a single equation. The resulting set of equations describing equilibria is under-determined, so solutions form a 1-manifold (curve) rather than points. This leads to situations where the post-disturbance behaviour of a wind turbine settles to a steady-state point that does not match pre-disturbance equilibrium conditions. The paper shows that such a mismatch will occur if the duplicate integrators do not switch synchronously. On the other hand, if synchronous switching is enforced, then pre- and post-disturbance equilibria will exactly match. These results have been illustrated using a standard WECC test case.

References

[1] Z. Lubosny, *Wind Turbine Operation in Electric Power Systems*. Springer, 2003.

[2] T. Ackermann (Editor), *Wind Power in Power Systems*. England: John Wiley and Sons, 2005.
[3] D. Kosterev and D. Davies, "System model validation studies in WECC," in *Proceedings of the IEEE PES General Meeting*, Minneapolis, MN, July 2010.
[4] J. Slootweg, S. de Haan, H. Polinder, and W. Kling, "General model for representing variable speed wind turbines in power system dynamics simulations," *IEEE Transactions on Power Systems*, vol. 18, no. 1, pp. 144–151, February 2003.
[5] J. Ekanayake, L. Holdsworth, X.-G. Wu, and N. Jenkins, "Dynamic modeling of doubly fed induction generator wind turbines," *IEEE Transactions on Power Systems*, vol. 18, no. 2, pp. 803–809, May 2003.
[6] J. Rose and I. Hiskens, "Estimating wind turbine parameters and quantifying their effects on dynamic behavior," in *Proceedings of the IEEE PES General Meeting*, Pittsburgh, PA, July 2008.
[7] K. Clark, N. Miller, and J. Sanchez-Gasca, "Modeling of GE wind turbine-generators for grid studies," Version 4.4, GE Energy, September 2009.
[8] E. Muljadi, C. Butterfield, J. Conto, and K. Donoho, "ERCOT's dynamic model of wind turbine generators," in *Proceedings of WindPower 2005*, Denver, CO, May 2005.
[9] "Generic type-3 wind turbine-generator model for grid studies," Version 1.1, WECC Wind Generator Modeling Group, September 2006.
[10] "WECC wind power plant dynamic modeling guide," WECC Renewable Energy Modeling Task Force, November 2010.
[11] I. Hiskens, "Trajectory deadlock in power system models," in *Proceedings of the IEEE International Symposium on Circuits and Systems*, Rio de Janeiro, Brazil, May 2011, pp. 2721–2724.
[12] ——, "Dynamics of type-3 wind turbine generator models," *IEEE Transactions on Power Systems*, vol. 27, no. 1, pp. 465–474, February 2012.
[13] A. Abate, A. D'Innocenzo, M. Di Benedetto, and S. Sastry, "Understanding deadlock and livelock behaviors in hybrid control systems," *Nonlinear Analysis: Hybrid Systems*, vol. 3, no. 2, pp. 150–162, May 2009.

Ian A. Hiskens (Fellow, IEEE) received the B.Eng. degree in electrical engineering and the B.App.Sc. degree in mathematics from the Capricornia Institute of Advanced Education, Rockhampton, Australia, in 1980 and 1983 respectively, and the Ph.D. degree in electrical engineering from the University of Newcastle, Australia, in 1991.

He is the Vennema Professor of Engineering in the Department of Electrical Engineering and Computer Science, University of Michigan, Ann Arbor. He has held prior appointments in the Queensland electricity supply industry, and various universities in Australia and the United States. His major research interests lie in the area of power system analysis, in particular system dynamics and control, and security assessment. His recent activity has focused largely on integration of renewable generation and controllable load.

Dr. Hiskens is actively involved in various IEEE societies, and is VP-Finance of the IEEE Systems Council. He is a Fellow of the IEEE, a Fellow of Engineers Australia and a Chartered Professional Engineer in Australia.